

Chiral symmetry and the nucleon-nucleon interaction: Tensor decomposition of Feynman diagrams

L. S. Celenza, A. Pantziris, and C. M. Shakin

*Department of Physics and Center for Nuclear Theory, Brooklyn College of The City University of New York,
Brooklyn, New York 11210*

(Received 30 April 1992)

A class of Lagrangians that describe the interaction of nucleons and pions and that provide a non-linear representation of chiral symmetry is considered. We simplify the form of these Lagrangians by making an expansion in inverse powers of f_π and calculate the *irreducible* fermion-fermion scattering amplitude to order f_π^{-4} . Some of the integrals encountered in these calculations are divergent and are regulated with a (Euclidean) momentum-space cutoff, Λ , where $\Lambda \simeq 1$ GeV. While elements of the S matrix are independent of the form of the Lagrangian used, somewhat different results are obtained for the *irreducible* amplitudes calculated with Lagrangians that have either pseudoscalar or pseudovector coupling of the pion field to the nucleon. We compare our results for the isoscalar irreducible amplitudes to the potentials used in the one-boson-exchange model of the nucleon-nucleon force. In the case of pseudovector coupling, there is only a single relevant diagram of order g^4 , a “crossed-box” diagram. We find that this crossed-box diagram is well represented by the exchange of a “pseudo-eta” particle, that is, an isoscalar-pseudoscalar meson with an imaginary coupling constant. There is also a relatively small scalar attraction seen, while tensor, vector, and axial vector terms are quite small. We also consider a Lagrangian with pseudoscalar coupling. In this case, there are four diagrams of order g^4 in the irreducible amplitude. Again, we find a significant attractive pseudoscalar exchange term (“pseudo-eta”). Relatively small repulsive interactions of vector and scalar type are also found in this case. Further analysis of the isoscalar amplitude requires that we extend our model to reproduce the dynamics of correlated two-pion exchange.

PACS number(s): 21.30.+y, 13.75.Cs, 24.80.Dc, 11.30.Rd

I. INTRODUCTION

One of the most useful representations of the nucleon-nucleon interaction is to be found in the one-boson-exchange model [1,2]. A good fit to nucleon-nucleon scattering and bound-state properties is obtained by considering the exchange of a number of mesons ($\sigma, \omega, \pi, \rho, \dots$). As is well known, the pion accounts for the longest range part of the force, while the pion and the ρ give rise to the nucleon-nucleon tensor interaction. The intermediate-range attraction may be described as arising from scalar meson exchange. However, since one does not find a scalar meson with a mass of about 550–600 MeV in the table of known particles and resonances, that meson is often said to be “fictitious.”

In order to understand the origin of the intermediate-range attraction, a number of studies that make use of dispersion relations have been performed [3,4]. These works suggest that a major part of the intermediate-range attraction arises from *correlated* two-pion-exchange processes. (We note that “correlated” two-pion exchange refers to those processes in which the pions undergo rescattering as they are exchanged. See Fig. 3 of Ref. [1], for example.) The studies that make use of dispersion relations differ somewhat in how they implement the constraints that arise from chiral symmetry. For example, in Ref. [4], use is made of a linear σ model, with a large mass for the σ field ($m_\sigma \geq 950$ MeV), in order to fit the pion-pion scattering amplitude. The success of that analysis, with a large value for the mass of the chiral partner of the pion, leads the authors of Ref. [4] to con-

clude that the scalar-isoscalar attraction in the nucleon-nucleon force does not arise from the exchange of the scalar field that is the chiral partner of the pion.

Although the study of dispersion relations leads to the notion that the fictitious σ (of mass of about 600 MeV) is an *effective field* related to correlated two-pion exchange, the precise relation of that result to Lagrangians that exhibit chiral symmetry is not clarified. On the other hand, the need to use a large value for the scalar mass in a *linear* chiral model [4] suggests that it is a nonlinear chiral model that may be most relevant to these studies. The nonlinear chiral models do not contain a scalar field in the Lagrangian and therefore, the origin of the intermediate-range attraction in the nucleon-nucleon force is not easily seen in such models. In this connection, we should also mention work based upon the Nambu–Jona-Lasinio model [5]. There, a scalar field appears as a broad $\bar{q}q$ resonance with a mass equal to twice the constituent quark mass generated when the chiral symmetry is broken. This scalar field may have some relation to the effective scalar field inferred from the study of dispersion relations. However, that matter has not been clarified and it appears that there is no general consensus as to the nature of the scalar attraction in the nucleon-nucleon force, or of the related scalar field that appears in various field-theoretic models of nuclear structure [6].

Recently, we have seen the development of a body of work that discusses the behavior of the quark condensate at finite baryon density, that is, in nuclear matter [7,10]. The quark condensate is found to decrease from its vacu-

um value by about 25–40 %, depending upon the size of the nucleon sigma term σ_N . The precise value of σ_N is unknown; however, recent studies yield $\sigma_N = 45 \pm 8$ MeV [11]. It was found useful to introduce a scalar order parameter $\bar{\sigma}$ that has value f_π in vacuum. Thus one may write $\bar{\sigma} = f_\pi + \sigma$, where σ is linearly dependent on the baryon density [7],

$$\sigma = -\frac{\sigma_N \rho_B}{m_\pi^2 f_\pi}. \quad (1.1)$$

If $\sigma_N = 50$ MeV we have $\sigma = -36$ MeV, which is close to the strength of the scalar field in the Serot and Walecka model [12] in Dirac phenomenology [13] and in relativistic Brueckner–Hartree-Fock theory [14]. The scalar potential is then $U_s = G_{\sigma NN} \sigma \simeq -340$ MeV, if we use $G_{\sigma NN} = 9.45$ [1,2].

These observations lead us to conclude that the scalar potentials used in the various models mentioned above reflect a partial restoration of chiral symmetry at finite baryon density [7–10]. Since a scalar potential of about $U_s = \simeq -390$ MeV is readily obtained when making use of the one-boson-exchange model of nuclear forces [1,2], it would appear that the scalar-isoscalar nucleon-nucleon interaction should be understood in a model that emphasizes the broken chiral symmetry of the underlying field theory. However, the generally accepted interpretation of the scalar part of the NN interaction is that it has its origin, in the main, in correlated two-pion exchange [3,4]. That interpretation does not provide a direct understanding of the relation between the NN interaction and relativistic nuclear physics.

Therefore, in this work we are interested in the role of chiral symmetry in the construction of models of the nucleon-nucleon force. However, it is clear that there are a number of ambiguities if a relativistic formalism is used to describe nucleon-nucleon scattering. For example, there is the question as to which relativistic equation is to be used. Once an equation is chosen, one must choose a procedure for the construction of a potential that is to be inserted in the equation. Here, we wish to understand aspects of the one-boson-exchange model of nuclear forces and will, therefore, describe the calculational procedure used in that model. In the simplest scheme, one parametrizes an irreducible amplitude in terms of the exchange of various bosons ($\sigma, \omega, \pi, \rho, \dots$) and obtains a unitary S matrix by solving a three-dimensional equation of the Blankenbecler-Sugar type, for example [1,2]. [If one contemplates using the Bethe-Salpeter equation as the fundamental relativistic equation, there are corrections to this procedure that depend on the difference of the two-nucleon (Feynman) propagators of the Bethe-Salpeter equation and the Blankenbecler-Sugar propagator. However, such corrections are not usually calculated. Therefore, the form of the phenomenological irreducible kernel may have some dependence on the reduction scheme used to go from a four-dimensional to a three-dimensional relativistic equation.] Further, it is worth noting that the one-boson-exchange models are usually evaluated in a “ladder approximation.” Therefore, in a phenomenological study of the nucleon-nucleon force

based on the one-boson-exchange model, it is not possible to describe the correlated two-pion-exchange process, except in terms of the exchange of an *effective* meson field, such as a σ meson. That meson is usually taken to have a mass of about 550–600 MeV in phenomenological studies [1,2].

We should also note that the role of chiral symmetry in the nucleon-nucleon interaction may also be studied by investigating the scattering of chiral solitons such as the Skyrmion [15]. However, one does not expect that the scalar attraction can be obtained in a mean-field approximation. Therefore, obtaining a scalar attraction in the Skyrme model requires a rather complex procedure. Some progress in this area has already been made [15].

In this work, we will calculate an irreducible nucleon-nucleon scattering amplitude, making use of Lagrangians that provide a nonlinear realization of chiral symmetry. (There are an infinite number of such Lagrangians that are related by chiral transforms and that have equivalent S matrices. The specific forms used here will be described in the next section.) As a first step in our program we will here study the isoscalar nucleon-nucleon interaction at one-loop order. (That is, we will complete a single four-dimensional integral in the calculation of each of the Feynman diagrams considered here.) In order to extend this work we should study correlated two-pion exchange. That feature has been studied most recently in Ref. [4], where use is made of dispersion relations to relate the $NN \rightarrow NN$ amplitude to the $\bar{N}N \rightarrow \pi\pi$ amplitude. The later amplitude is expressed in terms of the $\pi\pi \rightarrow \pi\pi$ amplitude and chiral symmetry is used in the construction of a model for that amplitude. While we have not as yet extended our analysis to study correlated two-pion exchange, we remark that some of the approximations of Ref. [4] may be useful in that enterprise. It may also be useful to study the Nambu–Jona-Lasinio model, which is equivalent to a linear σ model. The scalar (σ) meson of that model will mix strongly with the two-pion sector and may play a role in what is usually called “correlated two-pion exchange.”

The organization of our work is as follows. In Sec. II, we describe the Lagrangian to be used in this work and in Sec. III we provide a description of the calculational procedure in the case where pseudoscalar pion-nucleon coupling is adopted. In Sec. IV, we discuss the nucleon-nucleon interaction in the case where we use a Lagrangian with pseudovector pion-nucleon coupling. Results of our numerical calculations are presented in Sec. V. Section VI contains some further discussion and some conclusions.

II. PION-NUCLEON LAGRANGIAN

We consider a Lagrangian that possesses a chiral $SU(2)_L \times SU(2)_R$ symmetry that is spontaneously broken down to its $SU(2)_V$ subgroup, thus giving rise to a massless Goldstone boson, the pion field $\pi(x) = \pi(x) \cdot \tau$. One convenient nonlinear representation of the symmetry is obtained by use of the matrix $\Sigma = \exp[i\pi/f_\pi]$, where f_π is the pion decay constant $f_\pi = 93$ MeV. As noted above, there are infinitely many other representations that are

equivalent in the sense that they result in identical on-shell S -matrix elements (to all orders in perturbation theory). To lowest order in the number of derivatives of Σ , the effective Lagrangian for the pion-nucleon system is

$$\begin{aligned} \mathcal{L} = & i\bar{N}\not{\partial}N - M(\bar{N}_L\Sigma N_R + \bar{N}_R\Sigma^\dagger N_L) \\ & + i\lambda(\bar{N}_L\Sigma\not{\partial}\Sigma^\dagger N_L + \bar{N}_R\Sigma^\dagger\not{\partial}\Sigma N_R) \\ & + \frac{1}{4}f_\pi^2\text{Tr}[\partial_\mu\Sigma\partial^\mu\Sigma^\dagger]. \end{aligned} \quad (2.1)$$

Here M is the nucleon mass, as can be seen by expanding the exponentials. We also introduce a pion mass μ by adding the term

$$\frac{1}{4}\mu^2 f_\pi^2 \text{Tr}(\Sigma + \Sigma^\dagger), \quad (2.2)$$

which breaks the chiral symmetry of the Lagrangian explicitly.

The Lagrangian of Eq. (2.1) is very complicated when expressed in terms of the pion fields. However, by choosing a suitable basis for the nucleon fields, the Lagrangian can be reduced to a simpler form [16]. To that effect, we rotate the nucleon spinors to a new basis, $N_L \rightarrow N'_L = U^\dagger N_L, N_R \rightarrow N'_R = U N_R$, where $U = e^{i\alpha\pi(x)}$ is a transformation matrix that depends on the pion field. Choosing $\alpha = (f_\pi)^{-1}$, the pion-nucleon interaction Lagrangian becomes, to lowest orders in a formal expansion in $1/f_\pi$,

$$\mathcal{L}_{\pi NN}^{\text{PV}} \simeq -M\bar{N}N + \frac{2\lambda - 1}{2f_\pi} \bar{N}\gamma_5\not{\partial}\pi N + \frac{i}{8f_\pi^2} \bar{N}[\pi, \not{\partial}\pi]N. \quad (2.3)$$

Note that in this case, the lowest-order coupling is pseudovector. We can obtain pseudoscalar coupling by setting $\alpha = 2\lambda/f_\pi$. Then, the pion-nucleon Lagrangian becomes (to order $1/f_\pi^2$)

$$\begin{aligned} \mathcal{L}_{\pi NN}^{\text{PS}} \simeq & -M\bar{N}N + iM\frac{2\lambda - 1}{f_\pi} \bar{N}\gamma_5\pi N \\ & + \frac{1}{2}M \left[\frac{2\lambda - 1}{f_\pi} \right]^2 \bar{N}\pi^2 N \\ & + \frac{i\lambda(1 - \lambda)}{2f_\pi^2} \bar{N}[\pi, \not{\partial}\pi]N. \end{aligned} \quad (2.4)$$

(For complete expressions, and for arbitrary α , see Ref. [16].) In the following, we will consider both pseudoscalar and pseudovector coupling, although $\mathcal{L}_{\pi NN}^{\text{PS}}$ and $\mathcal{L}_{\pi NN}^{\text{PV}}$ are equivalent and yield identical on-shell matrix elements to order $1/f_\pi^4$. The parameter λ in Eqs. (2.1), (2.3), and (2.4) is chosen so as to reproduce the empirical value of the pion-nucleon coupling constant. Thus we have

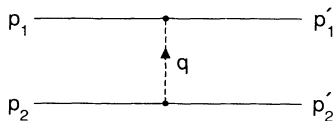


FIG. 1. Feynman diagram representing the direct term of single-pion exchange.

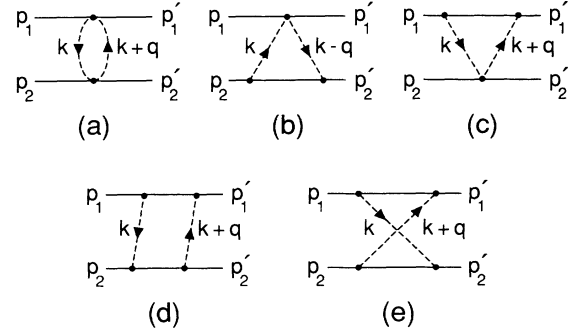


FIG. 2. Feynman diagrams for two-pion exchange (direct terms): (a) two-point loop, (b) and (c) three-point loops, (d) box diagram, and (e) crossed-box diagram.

$$g_{\pi NN} = (1 - 2\lambda) \frac{M}{f_\pi}. \quad (2.5)$$

The effective chiral Lagrangian of Eq. (2.4) can be used to evaluate the nucleon-nucleon scattering amplitude through one- and two-pion exchange. The one-pion-exchange amplitude, shown diagrammatically in Fig. 1, finds a natural place in the one-boson-exchange potential (OBEP) model of nuclear forces. The two-pion-exchange amplitude, however, consists of several terms (see Fig. 2) and is rather complicated.

It can be shown [17] that this amplitude, M , can, in general, be expressed in terms of five independent amplitudes (Fermi invariants), denoted by

$$S = [\bar{u}(p'_1)u(p_1)][\bar{u}(p'_2)u(p_2)], \quad (2.6)$$

$$P = [\bar{u}(p'_1)\gamma_5 u(p_1)][\bar{u}(p'_2)\gamma_5 u(p_2)], \quad (2.7)$$

$$V = [\bar{u}(p'_1)\gamma_\mu u(p_1)][\bar{u}(p'_2)\gamma^\mu u(p_2)], \quad (2.8)$$

$$A = [\bar{u}(p'_1)\gamma_\mu\gamma_5 u(p_1)][\bar{u}(p'_2)\gamma^\mu\gamma_5 u(p_2)], \quad (2.9)$$

$$T = [\bar{u}(p'_1)\sigma_{\mu\nu}u(p_1)][\bar{u}(p'_2)\sigma^{\mu\nu}u(p_2)], \quad (2.10)$$

such that

$$iM = V_{(S)}S + V_{(P)}P + V_{(V)}V + V_{(A)}A + V_{(T)}T. \quad (2.11)$$

The potentials $V_{(i)}$ are functions of the Mandelstam variables s and t and can have both isoscalar and isovector parts

$$V_{(j)} = V_{(j)}^0 + V_{(j)}^1\tau_1 \cdot \tau_2. \quad (2.12)$$

It is the purpose of this work to construct these potentials in the isoscalar sector ($V_{(i)}^0$) and compare them with the empirical potentials needed in the one-boson-exchange model of nuclear forces.

III. NUCLEON-NUCLEON INTERACTION

We now consider the various exchange processes, shown in Fig. 2, that arise in the study of the pseudoscalar pion-nucleon interaction described by $\mathcal{L}_{\pi NN}^{\text{PS}}(x)$. [We note that the four-point vertices in Figs. 2(a)–2(c) can be of two types.] In Figs. 1 and 2, we have shown only the direct amplitudes. Throughout this work we will restrict

our analysis to the direct terms, but as will become obvious, our conclusions hold for the exchange terms as well. In addition, for simplicity, we will omit the initial- and final-state spinors, since they are external constants; their presence is implicit in our calculations.

The Lagrangian of Eq. (2.1) and the (approximate) Lagrangian of Eq. (2.4) are not renormalizable and are to be thought of as *effective* Lagrangians, valid only up to some mass scale. Above that scale, the effective theory breaks down and the underlying quark and gluon fields are then the relevant degrees of freedom. Note that the diagram of Fig. 2(a) is logarithmically divergent and requires some regularization scheme. In our analysis, we use a covariant (Euclidean) momentum cutoff Λ , although one could equally well use some suitable pion-nucleon form factors to limit the integration to the relevant physical region. We prefer the cutoff technique, since it provides a uniform treatment of all types of vertices. Physical arguments concerning the chiral symmetry breaking scale suggest a value for Λ of about 1 GeV [18]. We will discuss the dependence of our results on the choice of Λ in Sec. V. (Note that Λ is the only free parameter in our calculations.)

A. Two-point-loop diagram

This diagram is depicted in Fig. 2(a) and contains two four-point vertices. As noted above, these vertices can be of two types. Let us first examine the isospin structure of the four terms that are represented by this diagram. If both vertices are of type II corresponding to the $\bar{N}\pi^2N$ term in the Lagrangian (see caption of Fig. 3), the isospin factor is

$$I_1 = \delta_{\alpha\beta}(1)\delta_{\beta\alpha}(2) \quad (3.1a)$$

$$= 3, \quad (3.1b)$$

and the diagram represents an isoscalar process. If both vertices are of type III, the isospin factor is

$$I_2 = -i\varepsilon^{\alpha\beta\gamma}\tau_\gamma(1)[-i\varepsilon^{\alpha\beta\delta}\tau_\delta(2)] \quad (3.2a)$$

$$= -2\tau(1)\cdot\tau(2), \quad (3.2b)$$

and the resulting term is isovector. When the two vertices are of different type, the value for the diagram is zero:

$$I_{3,4} = \delta_{\alpha\beta}(1)[-i\varepsilon^{\alpha\beta\gamma}\tau_\gamma(2)] \quad (3.3a)$$

$$= 0. \quad (3.3b)$$

Therefore, only I_1 is of the desired type. In that case, our calculation yields for the full amplitude

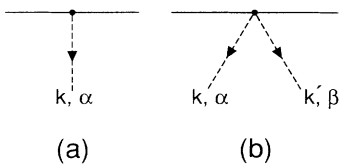


FIG. 3. (a) Diagrammatic representation of a vertex of type I. (b) Diagrammatic representation of a vertex of type II or type III.

$$I_1^{\text{PS}}(q^2) = -\frac{3M^2}{2f_\pi^4}(1-2\lambda)^4 \int \frac{d^4k}{(2\pi)^4} G(k)G(k+q), \quad (3.4)$$

where

$$G(k) = \frac{i}{k^2 - \mu^2 + i\varepsilon} \quad (3.5)$$

is the pion propagator. Thus, this diagram corresponds to a scalar interaction. Combining the denominators with Feynman parameters, we obtain

$$I_1^{\text{PS}}(q^2) = \frac{3iM^2}{32\pi^2 f_\pi^4} (1-2\lambda)^4 \times \int_0^1 dx \left\{ \ln \left[\frac{\Lambda^2 + A}{A} \right] - \frac{\Lambda^2}{\Lambda^2 + A} \right\}, \quad (3.6)$$

where $A = \mu^2 - q^2(x-x^2) - i\varepsilon$. For $q^2 < 0$, this expression is integrated analytically, yielding

$$I_1^{\text{PS}}(q^2) = \frac{3iM^2}{32\pi^2 f_\pi^4} (1-2\lambda)^4 \times \left\{ \Delta \ln \left[\frac{\Delta-1}{\Delta+1} \right] - \left[D + \frac{2\Lambda^2}{Dq^2} \right] \ln \left[\frac{D-1}{D+1} \right] + \ln \left[\frac{\Lambda^2 + \mu^2}{\mu^2} \right] \right\}, \quad (3.7)$$

where

$$\Delta = (1 - 4\mu^2/q^2)^{1/2} \quad (3.8)$$

and

$$D = \left[1 - 4 \frac{\Lambda^2 + \mu^2}{q^2} \right]^{1/2}. \quad (3.9)$$

Note that this diagram depends only on q^2 and, therefore, it is equivalent to a local potential. This is also the case for the three-point-loop diagrams, but not for the box and crossed-box diagrams.

B. Three-point-loop diagrams

These diagrams are shown in Figs. 2(b) and 2(c) and contain one four-point vertex and two ordinary pion-nucleon vertices. If the four-point vertex is of type II, the isospin factor is

$$I_1 = \delta_{\alpha\beta}(2)\tau_\alpha(1)\tau_\beta(1) \quad (3.10a)$$

$$= 3, \quad (3.10b)$$

and the diagram is isoscalar. If the four-point vertex is of type III, the isospin factor is

$$I_2 = [-i\varepsilon^{\alpha\beta\gamma}\tau_\gamma(2)]\tau_\alpha(1)\tau_\beta(1) \quad (3.11a)$$

$$= -i\varepsilon^{\alpha\beta\gamma}\tau_\gamma(2)[\delta_{\alpha\beta}(1) + i\varepsilon^{\alpha\beta\delta}\tau_\delta(1)] \quad (3.11b)$$

$$= 2\tau(1)\cdot\tau(2), \quad (3.11c)$$

and corresponds to an isovector process. Here, we only

consider the isoscalar process. Note that the diagrams of Figs. 2(b) and 2(c) give identical results, since they depend only on q^2 . The process of Fig. 2(b) is represented

$$I_2^{\text{PS}}(q^2) = i \frac{3M^3}{f_\pi^4} (1-2\lambda)^4 \int \frac{d^4k}{(2\pi)^4} G(k)G(k-q)\gamma_5 \times D(p_2-k)\gamma_5, \quad (3.12)$$

where $D(p)$ is the nucleon propagator

$$D(k) = \frac{i}{\not{p} - M + i\epsilon}. \quad (3.13)$$

Equation (3.12) can be easily simplified to give

$$I_2^{\text{PS}}(q^2) = -3 \frac{M^3}{f_\pi^4} (1-2\lambda)^4 \int \frac{d^4k}{(2\pi)^4} \frac{G(k)G(k-q)}{k^2 - 2p_2 \cdot k + i\epsilon} \times k^\mu \gamma_\mu. \quad (3.14)$$

As before, we combine denominators using Feynman parameters. The resulting denominator is

$$D = [k^2 - 2k \cdot (p_2x + qy) + (x\mu^2 + yq^2 - \mu^2 + i\epsilon)]^3. \quad (3.15)$$

By shifting the momentum integration variable

$$k^\mu \rightarrow k^\mu + xp^\mu + yq^\mu, \quad (3.16)$$

we complete the square in D . Then, the term linear in k^μ vanishes (since it is odd in k), as does the term linear in q^μ , since \not{q} vanishes between the on-shell spinors. Thus, only the term proportional to xp_2^μ survives and, since \not{p}_2 may be replaced by M , when \not{p}_2 is found between the spinors, the result is of purely scalar form:

$$I_2^{\text{PS}}(q^2) = -\frac{3iM^4}{16\pi^2 f_\pi^4} (1-2\lambda)^4 \times \int_0^1 dy \int_0^{1-y} dx \frac{x}{A} \left[\frac{\Lambda^2}{\Lambda^2 + A} \right]^2, \quad (3.17)$$

where

$$A = y(x+y-1)q^2 + x^2M^2 + (1-x)\mu^2 - i\epsilon. \quad (3.18)$$

We can perform the integral over the x variable analytically, but the result is a rather long expression and is not given here.

C. Box and crossed-box diagrams

The box and crossed-box diagrams, shown in Figs. 2(d) and 2(e), respectively, are related by a change of variables and therefore, we analyze them together. We first discuss the isospin factors. For the box diagram

$$I = [\tau_\alpha(1)\tau_\beta(1)][\tau_\alpha(2)\tau_\beta(2)] \quad (3.19a)$$

$$= 3 - 2\tau(1) \cdot \tau(2), \quad (3.19b)$$

while for the crossed-box diagram

$$I = [\tau_\alpha(1)\tau_\beta(1)][\tau_\beta(2)\tau_\alpha(2)] \quad (3.20a)$$

$$= 3 + 2\tau(1) \cdot \tau(2). \quad (3.20b)$$

Thus both of these diagrams have an isoscalar and an isovector part. The isoscalar parts of the box and crossed-box diagrams are expressed as

$$I_3^{\text{PS}}(q^2, p_1 \cdot p_2) = 3 \frac{M^4}{f_\pi^4} (1-2\lambda)^4 \int \frac{d^4k}{(2\pi)^4} G(k)G(k-q) \times [\gamma_5 D(p_1-k)\gamma_5]_{(1)} \times [\gamma_5 D(p_2+k)\gamma_5]_{(2)} \quad (3.21)$$

and

$$I_4^{\text{PS}}(q^2, p_1 \cdot p_2) = 3 \frac{M^4}{f_\pi^4} (1-2\lambda)^4 \int \frac{d^4k}{(2\pi)^4} G(k)G(k-q) \times [\gamma_5 D(p_1-k)\gamma_5]_{(1)} \times [\gamma_5 D(p_2'-k)\gamma_5]_{(2)}, \quad (3.22)$$

respectively. The indices (1) and (2) refer to the first and second nucleon lines. It is most convenient to express I_3 and I_4 in terms of q ,

$$\pi_1 = \frac{1}{2}(p_1 + p_1') \quad (3.23)$$

and

$$\pi_2 = \frac{1}{2}(p_2 + p_2'). \quad (3.24)$$

We also change variables ($k \rightarrow k - q/2$), in which case the integrals of Eqs. (3.21) and (3.22) can be brought into the symmetric forms,

$$I_3^{\text{PS}} = 3 \frac{M^4}{f_\pi^4} (1-2\lambda)^4 \times \int \frac{d^4k}{(2\pi)^4} \frac{G(k+q/2)G(k-q/2)}{[(k-\pi_1)^2 - M^2][(k+\pi_2)^2 - M^2]} \times k^\mu k^\nu \gamma_\mu(1)\gamma_\nu(2) \quad (3.25)$$

and

$$I_4^{\text{PS}} = -3 \frac{M^4}{f_\pi^4} (1-2\lambda)^4 \times \int \frac{d^4k}{(2\pi)^4} \frac{G(k+q/2)G(k-q/2)}{[(k-\pi_1)^2 - M^2][(k-\pi_2)^2 - M^2]} \times k^\mu k^\nu \gamma_\mu(1)\gamma_\nu(2), \quad (3.26)$$

after performing some Dirac algebra.

We now combine the four denominators to a single one. The denominator can be written as

$$D = [k^2 - 2k \cdot p - B^2]^4, \quad (3.27)$$

where

$$p_{(3)}^\mu = y\pi_1^\mu - x\pi_2^\mu + \frac{1}{2}(x+y+2z-1)q^\mu \quad (3.28)$$

and

$$p_{(4)}^\mu = y\pi_1^\mu + x\pi_2^\mu + \frac{1}{2}(x+y+2z-1)q^\mu, \quad (3.29)$$

$$B^2 = (1-x-y)(\mu^2 - q^2/4) + (x+y)q^2/4. \quad (3.30)$$

Here $p_{(3)}^\mu$ and $p_{(4)}^\mu$ are the momenta that appear in Eq. (3.27) for the case of the box and crossed-box diagrams, respectively. The tensor integral can be reduced to a scalar one. The second term of this equation, proportional to $g^{\mu\nu}$, leads to a term that is of the form $\gamma^\mu(1)\gamma_\mu(2)$, describing a pure vector interaction. The remaining term, proportional to $p^\mu p^\nu$, requires further analysis. The terms that are proportional to q^μ and/or q^ν do not contribute, since $q^\mu\gamma_\mu(1) = q^\nu\gamma_\nu(2) = 0$, when these expressions are found between the spinors. Only the terms proportional to $p_1^\mu p_1^\nu$, $p_1^\mu p_2^\nu$, $p_2^\mu p_1^\nu$, and $p_2^\mu p_2^\nu$ contribute. We exhibit the various tensorial parts of these terms. For the operator $p_{(3)}^\mu\gamma_\mu(1)p_{(3)}^\nu\gamma_\nu(2)$ they are

$$F_{(3)}^{(S)} = \frac{1}{2}\pi_1 \cdot \pi_2 (x^2 + y^2) - M^2 xy, \quad (3.31)$$

$$F_{(3)}^{(P)} = F_{(3)}^{(S)}, \quad (3.32)$$

$$F_{(3)}^{(V)} = \frac{1}{2}M^2(x^2 + y^2) - \pi_1 \cdot \pi_2 xy, \quad (3.33)$$

$$F_{(3)}^{(A)} = -\frac{1}{4}q^2 xy, \quad (3.34)$$

$$F_{(3)}^{(T)} = \frac{1}{4}q^2(x^2 + y^2), \quad (3.35)$$

while for the operator $p_{(4)}^\mu\gamma_\mu(1)p_{(4)}^\nu\gamma_\nu(2)$, we obtain

$$F_{(4)}^{(S)} = \frac{1}{2}\pi_1 \cdot \pi_2 (x^2 + y^2) - M^2 xy, \quad (3.36)$$

$$F_{(4)}^{(P)} = F_{(4)}^{(S)}, \quad (3.37)$$

$$F_{(4)}^{(V)} = \frac{1}{2}M^2(x^2 + y^2) + \pi_1 \cdot \pi_2 xy, \quad (3.38)$$

$$F_{(4)}^{(A)} = \frac{1}{4}q^2 xy, \quad (3.39)$$

$$F_{(4)}^{(T)} = -\frac{1}{4}q^2(x^2 + y^2). \quad (3.40)$$

Then the various pieces $I_3^{\text{PS}(j)}$ of the box diagram for $j=S, P, A$, and T can be written as

$$I_3^{\text{PS}(j)} = -\frac{3iM^4\Lambda^4}{16\pi^2 f_\pi^4} (1-2\lambda)^4 \times \int_0^1 dz \int_0^{1-z} dy \int_0^{1-z-y} dx \frac{\Lambda^2 + 3A}{(\Lambda^2 + A)^3 A^2} \times F_{(3)}^{(j)}, \quad (3.41)$$

where $A = B^2 + p_{(3)}^2$. The vector part contains the additional term proportional to $g^{\mu\nu}$, thus

$$I_3^{\text{PS}(V)} = -\frac{3iM^4\Lambda^4}{16\pi^2 f_\pi^4} (1-2\lambda)^4 \int_0^1 dz \int_0^{1-z} dy \int_0^{1-z-y} dx \left[\frac{\Lambda^2 + 3A}{(\Lambda^2 + A)^3 A^2} F_{(3)}^{(V)} - \frac{1}{A(\Lambda^2 + A)^2} \right]. \quad (3.42)$$

Similar expressions can be written for the various pieces of the crossed-box diagram. Upon inspection, one can easily verify that

$$I_4^{\text{PS}(S)}(q^2, \pi_1 \cdot \pi_2) = I_3^{\text{PS}(S)}(q^2, -\pi_1 \cdot \pi_2), \quad (3.43)$$

$$I_4^{\text{PS}(P)}(q^2, \pi_1 \cdot \pi_2) = I_3^{\text{PS}(P)}(q^2, -\pi_1 \cdot \pi_2), \quad (3.44)$$

$$I_4^{\text{PS}(V)}(q^2, \pi_1 \cdot \pi_2) = -I_3^{\text{PS}(V)}(q^2, -\pi_1 \cdot \pi_2), \quad (3.45)$$

$$I_4^{\text{PS}(A)}(q^2, \pi_1 \cdot \pi_2) = I_3^{\text{PS}(A)}(q^2, -\pi_1 \cdot \pi_2), \quad (3.46)$$

$$I_4^{\text{PS}(T)}(q^2, \pi_1 \cdot \pi_2) = -I_3^{\text{PS}(T)}(q^2, -\pi_1 \cdot \pi_2). \quad (3.47)$$

The integrals of Eqs. (3.41)–(3.47) are then evaluated numerically. (Since we are calculating an *irreducible* amplitude, we do not require the results for the box diagram.)

IV. NUCLEON-NUCLEON INTERACTION: PSEUDOVECTOR COUPLING

The Lagrangian of Eq. (2.3) describes pseudovector pion-nucleon coupling to lowest order in f_π^{-1} . The Feyn-

man diagrams representing the nucleon-nucleon interaction via two-pion exchange are identical to those of the pseudoscalar case (shown in Fig. 2). However, there is only a single four-point vertex in this case of type III and, as shown in Eqs. (3.2) and (3.11), a type III vertex always yields an isovector nucleon-nucleon interaction. The only diagrams that have an isoscalar part are the box and crossed-box diagrams [Figs. 2(d) and 2(e)]. In both cases, the relevant isospin factor is equal to 3, as was shown in Eqs. (3.19) and (3.20).

Since the Lagrangians of Eqs. (2.3) and (2.4) are equivalent, the sum of all diagrams in each coupling scheme is identical, as long as we systematically calculate all terms up to order f_π^{-4} , for example. In fact, the sum of diagrams up to that order (or any other order) is an invariant quantity that does not depend on the particular realization of chiral symmetry used. However, since we are interested in separating the reducible and irreducible parts of the amplitude, we proceed to evaluate the box and crossed-box diagrams separately.

There is only one vertex to consider,

$$\Gamma_\alpha^{\text{PV}} = \frac{2\lambda - 1}{2f_\pi} \gamma_S \not{p} \tau_\alpha. \quad (4.1)$$

The box and crossed-box diagrams are given by

$$I_3^{\text{PV}} = 3 \left[\frac{2\lambda-1}{2f_\pi} \right]^4 \int \frac{d^4k}{(2\pi)^4} G(k)G(k-q) \times [\gamma_5(\not{q}-\not{k})D(p_1-k)\gamma_5\not{k}]_{(1)} \times [\gamma_5(\not{q}-\not{k})D(p_2+k)\gamma_5\not{k}]_{(2)} \quad (4.2)$$

$$I_4^{\text{PV}} = 3 \left[\frac{2\lambda-1}{2f_\pi} \right]^4 \int \frac{d^4k}{(2\pi)^4} G(k)G(k-q) \times [\gamma_5(\not{q}-\not{k})D(p_1-k)\gamma_5\not{k}]_{(1)} \times [\gamma_5\not{k}D(p_2'-k)\gamma_5(\not{q}-\not{k})]_{(2)}, \quad (4.3)$$

and

respectively. After simplifying the Dirac structure by commuting the γ_5 's, and using the on-shell character of the initial and final spinors, these amplitudes can be written as

$$I_3^{\text{PV}} = -3(4M^2) \left[\frac{2\lambda-1}{2f_\pi} \right]^4 \int \frac{d^4k}{(2\pi)^4} G(k)G(k-q) \left\{ 1 + \frac{\not{k}(1)}{2M} \left[1 + \frac{4M^2}{S(p_1-k)} \right] \right\} \left\{ 1 - \frac{\not{k}(2)}{2M} \left[1 + \frac{4M^2}{S(p_2+k)} \right] \right\} \quad (4.4)$$

and

$$I_4^{\text{PV}} = -3(4M^2) \left[\frac{2\lambda-1}{2f_\pi} \right]^4 \int \frac{d^4k}{(2\pi)^4} G(k)G(k-q) \left\{ 1 + \frac{\not{k}(1)}{2M} \left[1 + \frac{4M^2}{S(p_1-k)} \right] \right\} \left\{ 1 + \frac{\not{k}(2)}{2M} \left[1 + \frac{4M^2}{S(p_2'-k)} \right] \right\}, \quad (4.5)$$

where

$$S(p) = p^2 - M^2 + i\epsilon. \quad (4.6)$$

We now rewrite Eqs. (4.4) and (4.5) in a symmetric form by changing the integration variable ($k \rightarrow k' = k - q/2$) and expressing I_3^{PV} and I_4^{PV} in terms of π_1 and π_2 [see Eqs. (3.23) and (3.24)]. Using the symmetry under the change $k \rightarrow -k$, some terms are seen to vanish, and the amplitudes become

$$I_3^{\text{PV}} = -3(4M^2) \left[\frac{2\lambda-1}{2f_\pi} \right]^4 \int \frac{d^4k}{(2\pi)^4} G(k)G(k-q) \left\{ 1 + \frac{2M\not{k}(1)}{S(\pi_1-k)} - \frac{2M\not{k}(2)}{S(\pi_2+k)} - \frac{\not{k}(1)\not{k}(2)}{4M^2} \left[1 + \frac{4M^2}{S(\pi_1-k)} \right] \left[1 + \frac{4M^2}{S(\pi_2+k)} \right] \right\} \quad (4.7)$$

and

$$I_4^{\text{PV}} = -3(4M^2) \left[\frac{2\lambda-1}{2f_\pi} \right]^4 \int \frac{d^4k}{(2\pi)^4} G(k)G(k-q) \left\{ 1 + \frac{2M\not{k}(1)}{S(\pi_1-k)} + \frac{2M\not{k}(2)}{S(\pi_2-k)} + \frac{\not{k}(1)\not{k}(2)}{4M^2} \left[1 + \frac{4M^2}{S(\pi_1-k)} \right] \left[1 + \frac{4M^2}{S(\pi_2-k)} \right] \right\}. \quad (4.8)$$

An inspection of the results derived in Sec. III reveals that the box and crossed-box diagrams can be expressed as

$$I_3^{\text{PV}} = \frac{1}{2}[I_1^{\text{PS}} + 2I_2^{\text{PS}}] + I_3^{\text{PS}} + I_R \quad (4.9)$$

and

$$I_4^{\text{PV}} = \frac{1}{2}[I_1^{\text{PS}} + 2I_2^{\text{PS}}] + I_4^{\text{PS}} - I_R, \quad (4.10)$$

where

$$I_R = 3(4M^2) \left[\frac{2\lambda-1}{2f_\pi} \right]^4 \int \frac{d^4k}{(2\pi)^4} G(k)G(k-q) \not{k}(1)\not{k}(2) \times \left[\frac{1}{4M^2} + \frac{1}{S(\pi_1-k)} + \frac{1}{S(\pi_2+k)} \right]. \quad (4.11)$$

Note that as expected the sum of the pseudovector amplitudes is equal to the corresponding pseudoscalar sum:

$$I_3^{\text{PV}} + I_4^{\text{PV}} = I_1^{\text{PS}} + 2I_2^{\text{PS}} + I_3^{\text{PS}} + I_4^{\text{PS}}. \quad (4.12)$$

The integral of Eq. (4.11), I_R , is found to consist of three terms. The first term, $I_R^{(1)}$, is proportional to $1/(4M^2)$ and does not depend on π_1 or π_2 . Therefore, the integral can only be proportional to $g^{\mu\nu}\gamma_\mu(1)\gamma_\nu(2)$ (we recall that \not{q} vanishes between the spinors), and describes a purely vector interaction. We find

$$I_R^{(1)} = -\frac{3i}{64\pi^2 f_\pi^4} \left(\frac{1}{2}-\lambda\right)^4 \int_0^1 dx \left\{ 2A \ln \left[\frac{\Lambda^2 + A}{A} \right] - \frac{\Lambda^2(\Lambda^2 + 2A)}{\Lambda^2 + A} \right\}, \quad (4.13)$$

where

$$A = \mu^2 + q^2 x(x-1). \quad (4.14)$$

The other two terms can be shown to have equal con-

tribution. Therefore, we write $I_R = I_R^{(1)} + 2I_R^{(2)}$. The procedure used to calculate $I_R^{(2)}$ is similar to that used in the case of I_2^{PS} , except that, in this case, the integral is of tensor character. We find that

$$I_R^{(2)} = -\frac{3M^2}{2f_\pi^4} (1-2\lambda)^4 \int_0^1 dx_1 \int_0^{1-x_1} dx_2 \left\{ \int \frac{d^4k}{(2\pi)^4} \frac{k(1)k(2)}{(k^2-A)^3} + \mathcal{P}(1)\mathcal{P}(2) \int \frac{d^4k}{(2\pi)^4} \frac{1}{(k^2-A)^3} \right\}, \quad (4.15)$$

where

$$P^\mu = x_1 q^\mu + x_2 p_1^\mu \quad (4.16)$$

and

$$A = (1-x_2)\mu^2 - x_1 q^2 + P^2. \quad (4.17)$$

The first term in Eq. (4.15) is a pure vector interaction. The second term is proportional to $\mathcal{P}(1)\mathcal{P}(2)$ and therefore has several tensorial components $J_R^{(i)}$. Assuming that we will form spinor matrix elements, and using Eq. (4.16), we have

$$\mathcal{P}(1)\mathcal{P}(2) = x_2^2 M \not{p}_1(2). \quad (4.18)$$

A tensor decomposition of this term can be made [19,20]. The result for the various $J_R^{(i)}$ is then

$$J_R^{(j)} = \frac{3iM^2}{32\pi^2 f_\pi^4} (1-2\lambda)^4 \int_0^1 dx_1 \int_0^{1-x_1} dx_2 x_2^2 \frac{\Lambda^4}{A(\Lambda^2+A)^2} F_R^{(j)}, \quad (4.19)$$

where $j = S, P, A$, and T . The vector part is given by

$$I_R^{(V)} = I_R^{(1)} + \frac{3iM^2}{32\pi^2 f_\pi^4} (1-2\lambda)^4 \int_0^1 dx_1 \int_0^{1-x_1} dx_2 \left\{ x_2^2 \frac{\Lambda^4}{A(\Lambda^2+A)^2} F_R^{(V)} + \left[\frac{\Lambda^2(3\Lambda^2+2A)}{4(\Lambda^2+A)^2} - \frac{1}{2} \ln \frac{\Lambda^2+A}{A} \right] \right\}, \quad (4.20)$$

where

$$F_R^{(S)} = \frac{1}{2} \pi_1 \cdot \pi_2, \quad (4.21a)$$

$$F_R^{(P)} = F_R^{(S)}, \quad (4.21b)$$

$$F_R^{(V)} = \frac{1}{2} M^2, \quad (4.21c)$$

$$F_R^{(A)} = 0, \quad (4.21d)$$

$$F_R^{(T)} = -\frac{1}{4} q^2. \quad (4.21e)$$

We present results of the numerical evaluation of Eqs. (4.19) and (4.20) in the next section.

V. NUMERICAL RESULTS

Here, we present the results of the numerical evaluation of the various tensorial components of the integrals $I_1^{\text{PS}}(q^2)$, $I_2^{\text{PS}}(q^2)$, $I_3^{\text{PS}}(q^2, p_1 \cdot p_2)$, $I_4^{\text{PS}}(q^2, p_1 \cdot p_2)$, $I_3^{\text{PV}}(q^2, p_1 \cdot p_2)$, and $I_4^{\text{PV}}(q^2, p_1 \cdot p_2)$ as given by Eqs. (3.6), (3.17), (3.30), (3.41)–(3.47), (4.9), and (4.10). The pion-nucleon coupling constant used is such that $g_{\pi NN}^2/(4\pi) = 14.9$.

We define the potentials

$$V_j^{\text{PS}}(q^2) = iI_j^{\text{PS}}(q^2) \quad \text{for } j=1, \dots, 4, \quad (5.1)$$

$$V_j^{\text{PV}}(q^2) = iI_j^{\text{PV}}(q^2) \quad \text{for } j=3 \text{ and } 4, \quad (5.2)$$

and $V_\sigma(q^2)$, the scalar potential arising from σ -meson ex-

change in the one-boson-exchange model (direct term),

$$V_\sigma(q^2) = -\frac{g_{\sigma NN}^2}{m_\sigma^2 - q^2} \left[\frac{\Lambda_\sigma^2 - m_\sigma^2}{\Lambda_\sigma^2 - q^2} \right]^2. \quad (5.3)$$

The σ -nucleon coupling constant is taken to be $g_{\sigma NN}^2/(4\pi) = 8.31$, the σ mass is 0.55 GeV, and the form-factor cutoff is $\Lambda_\sigma = 2.0$ GeV. This corresponds to the potential A of Table A.2 in Ref. [2]. (Λ_σ should not be confused with the cutoff Λ .)

In Fig. 4 we plot the individual contributions $V_j^{\text{PS}}(q^2)$ and $V_j^{\text{PV}}(q^2)$ of the scalar components of the potentials for $\Lambda = 1.0$ GeV and for $s = 4M^2 + 0.3$ GeV². In the pseudoscalar coupling scheme, only $V_1^{\text{PS}}(q^2)$ varies appreciably with increasing Λ , as is expected, since $V_1^{\text{PS}}(q^2)$ diverges logarithmically as $\Lambda \rightarrow \infty$. Note also the strong cancellation between the various terms. In the pseudovector case, both $V_3^{\text{PV}}(q^2)$ and $V_4^{\text{PV}}(q^2)$ are logarithmically divergent with increasing Λ .

Our main interest lies in the *irreducible* part of the two-pion-exchange potential. In the pseudoscalar coupling scheme, the irreducible interaction is represented by the sum

$$V_{\text{irr}}^{\text{PS}}(q^2) = V_1^{\text{PS}}(q^2) + 2V_2^{\text{PS}}(q^2) + V_4^{\text{PS}}(q^2), \quad (5.4)$$

while in the pseudovector case, it is simply the contribution of the crossed-box diagram:

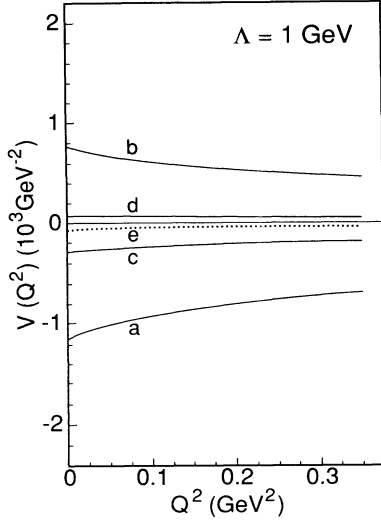


FIG. 4. Contributions of the various two-pion-exchange diagrams to the scalar potential for the pseudoscalar (solid lines) and pseudovector (dotted lines) coupling schemes: (a) $V_1^{\text{PS}(S)}(q^2)$ (two-point loop); (b) $V_2^{\text{PS}(S)}(q^2)$ (three-point loop); (c) $V_4^{\text{PS}(S)}(q^2)$ (crossed-box diagram); (d) $V_{\text{irr}}^{\text{PS}(S)}(q^2)$; and (e) $V_{\text{irr}}^{\text{PV}(S)}(q^2)$. [Here $\Lambda=1.0$ GeV, $g_\pi^2/(4\pi)=14.9$, and $Q^2=-q^2$.]

$$V_{\text{irr}}^{\text{PV}}(q^2) = V_4^{\text{PV}}(q^2). \quad (5.5)$$

Choosing the irreducible part of the potential (in either coupling scheme) excludes from the sum of all diagrams the contribution of the box diagram [$V_3^{\text{PS}}(q^2)$ or $V_3^{\text{PV}}(q^2)$], since that term will automatically be generated by the iteration of the Born term (one-pion exchange) in the Bethe-Salpeter equation. Therefore, the box diagram is automatically taken into account when constructing the scattering amplitude. Note, however, that the potentials $V_j(q^2)$ describe fully-on-shell amplitudes, while the solution of the Bethe-Salpeter equation requires the knowledge of the off-shell amplitude as well.

As can be seen in Fig. 4, because of the strong cancellations, $V_{\text{irr}}^{(s)}$ is much smaller than the contribution of the individual terms (in either coupling scheme) for $\Lambda=1.0$ GeV. Thus, it appears that the two-pion-exchange process does not lead to any appreciable scalar interaction at one-loop order and certainly cannot account for the empirical σ -meson potential of the one-boson-exchange model. At most, in the pseudovector coupling scheme, the uncorrelated two-pion exchange can reproduce about 25% of the empirical potential $V_\sigma(q^2)$, while in the pseudoscalar case it is small and repulsive. One should bear in mind however that for $\Lambda \rightarrow \infty$, both $V_{\text{irr}}^{\text{PS}(S)}$ and $V_{\text{irr}}^{\text{PV}(S)}$ are negative and diverge logarithmically, with [see Eq. (4.10)]

$$\lim_{\Lambda \rightarrow \infty} \frac{V_{\text{irr}}^{\text{PV}(S)}}{V_{\text{irr}}^{\text{PS}(S)}} = \frac{1}{2}. \quad (5.6)$$

In Fig. 5 we present the various tensorial components of the irreducible two-pion-exchange potential in the pseudoscalar coupling scheme for $\Lambda=1.0$ GeV. Here

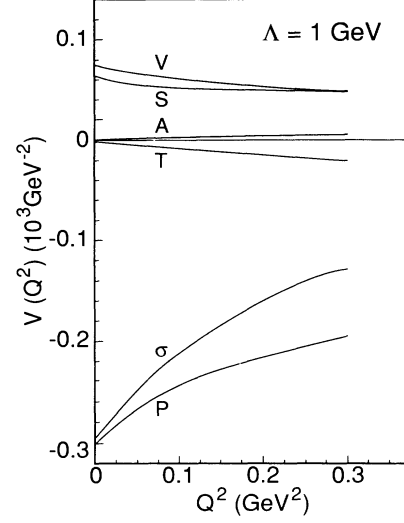


FIG. 5. Tensor components of the irreducible two-pion-exchange potential in the pseudoscalar coupling scheme at $\Lambda=1$ GeV. The potential $V_\sigma(q^2)$ is shown for comparison. Here $s=4M^2+0.3$ GeV 2 . (S) $V_{\text{irr}}^{\text{PS}(S)}$, (P) $V_{\text{irr}}^{\text{PS}(P)}$, (V) $V_{\text{irr}}^{\text{PS}(V)}$, (A) $V_{\text{irr}}^{\text{PS}(A)}$, (T) $V_{\text{irr}}^{\text{PS}(T)}$, and (σ) V_σ . (Here $Q^2=-q^2$.)

$s=4M^2+0.3$ GeV 2 , ensuring that the potentials are evaluated in the physical region if $0 \leq -t \leq 0.3$ GeV 2 . In this region, the irreducible potentials are real, but the box diagrams are not, except at the point $(s,t)=(0,0)$. We also plot, for comparison, the empirical σ potential $V_\sigma(q^2)$ of Eq. (5.3).

The main feature of Fig. 5 is the prediction of a large *attractive* pseudoscalar potential corresponding to a “pseudo- η ” exchange. The effect of such a potential would be to reduce the repulsive potential obtained if the observed $\eta(548.8)$ particle is included in the OBEP model. (The magnitude of $V_{\text{irr}}^{\text{PS}(P)}$ suggests that if one includes a physical η , the corresponding potential would be canceled by a contribution of the opposite sign arising from the cross-box diagram.) This feature provides an argument for the consistency of OBEP fits to nucleon-nucleon scattering data that do not include an η particle meson.

In addition, in Fig. 5, we observe some small vector and scalar repulsive potentials. However, their magnitude is much smaller than the corresponding potentials of the boson-exchange model that arise from ω and σ exchange. (To obtain larger σ -like potentials we will have to consider higher-order diagrams.) We also note that the axial vector and tensor components of the interaction are negligible in this (small t) region.

In Fig. 6, we give results of a calculation of $V_{\text{irr}}^{\text{PS}(i)}$ for $\Lambda=2.0$ GeV. Although the physically meaningful value for Λ is thought to be about 1 GeV, it is interesting to see how the results depend on the cutoff. We observe little change for $V_{\text{irr}}^{\text{PS}(P)}$, $V_{\text{irr}}^{\text{PS}(A)}$, and $V_{\text{irr}}^{\text{PS}(T)}$, as expected, since the corresponding integrals are finite as $\Lambda \rightarrow \infty$. The vector interaction $V_{\text{irr}}^{\text{PS}(V)}$ is more sensitive to Λ , since there are large cancellations in its calculation. A much larger change is observed for the scalar potential when increas-

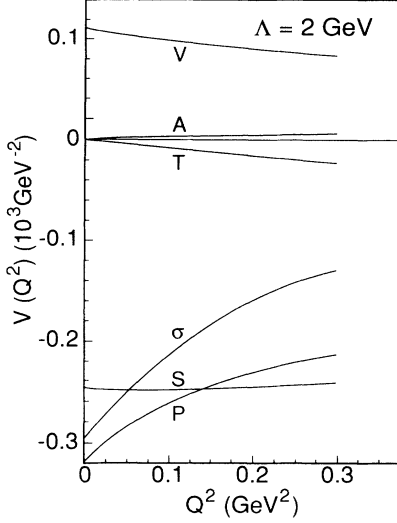


FIG. 6. Tensor components of the irreducible two-pion-exchange potential in the pseudoscalar coupling scheme at $\Lambda=2$ GeV. The potential $V_\sigma(q^2)$ is shown for comparison. Here $s=4M^2+0.3$ GeV 2 . (S) $V_{\text{irr}}^{\text{PS}(S)}$, (P) $V_{\text{irr}}^{\text{PS}(P)}$, (V) $V_{\text{irr}}^{\text{PS}(V)}$, (A) $V_{\text{irr}}^{\text{PS}(A)}$, (T) $V_{\text{irr}}^{\text{PS}(T)}$, and (σ) V_σ .

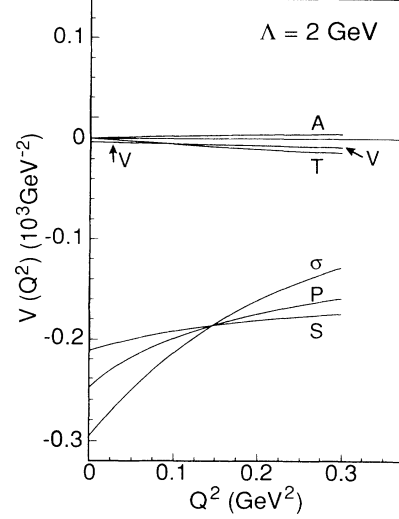


FIG. 8. Tensor components of the irreducible two-pion-exchange potential in the pseudovector coupling scheme for $\Lambda=2$ GeV. Here $s=4M^2+0.3$ GeV 2 . (S) $V_{\text{irr}}^{\text{PV}(S)}$, (P) $V_{\text{irr}}^{\text{PV}(P)}$, (V) $V_{\text{irr}}^{\text{PV}(V)}$, (A) $V_{\text{irr}}^{\text{PV}(A)}$, (T) $V_{\text{irr}}^{\text{PV}(T)}$, and (σ) V_σ .

ing Λ , since the corresponding integral is logarithmically divergent as $\Lambda \rightarrow \infty$.

In Fig. 7 we plot the various tensorial components of the irreducible potential in the case of the pseudovector coupling scheme for $\Lambda=1.0$ GeV and $s=4M^2+0.3$ GeV 2 . We observe that the two coupling schemes lead to similar qualitative results in most cases. Again, the main feature is the appearance of a “pseudo- η ” pseudoscalar potential with a mass parameter closer to that of the physical η particle than that found in the pseudoscalar coupling scheme. In Fig. 7 we also see that vector in-

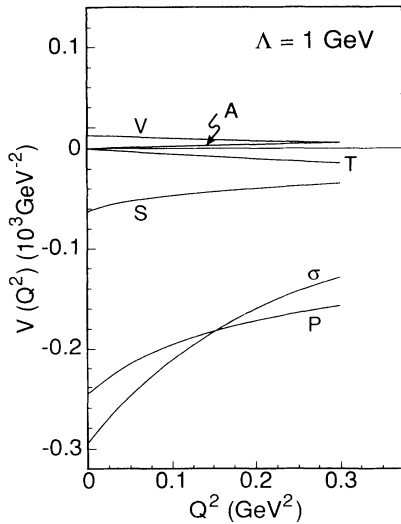


FIG. 7. Tensor components of the irreducible two-pion-exchange potential in the pseudovector coupling scheme for $\Lambda=1$ GeV. Here $s=4M^2+0.3$ GeV 2 . (S) $V_{\text{irr}}^{\text{PV}(S)}$, (P) $V_{\text{irr}}^{\text{PV}(P)}$, (V) $V_{\text{irr}}^{\text{PV}(V)}$, (A) $V_{\text{irr}}^{\text{PV}(A)}$, (T) $V_{\text{irr}}^{\text{PV}(T)}$, and (σ) V_σ .

teraction is negligible (again due to very large cancellations in its calculation). The axial vector and tensor interactions are again quite small.

We repeat the calculation of Fig. 7 for $\Lambda=2$ GeV and present the results in Fig. 8. As in the case of the pseudoscalar coupling scheme, $V_{\text{irr}}^{\text{PV}(P)}$, $V_{\text{irr}}^{\text{PV}(V)}$, $V_{\text{irr}}^{\text{PV}(A)}$, and $V_{\text{irr}}^{\text{PV}(T)}$ remain essentially unchanged, while the logarithmically divergent component $V_{\text{irr}}^{\text{PV}(S)}$ becomes comparable to $V_\sigma(q^2)$. The results shown in Fig. 7 suggest that some part of the scalar attraction associated with the σ meson of the boson-exchange model may have its origin in the two-pion-exchange potential if the pseudovector coupling scheme is used.

Since the sum $V_{\text{irr}} + V_{\text{red}}$ is the same in both coupling schemes, one should prefer the coupling scheme in which the reducible diagrams are best approximated within the reduction schemes used in the boson-exchange model. We have not undertaken such a study in the present work.

As we mentioned previously, we have only calculated the contribution of the direct diagrams of the two-pion-exchange process. In a similar fashion we can calculate the nucleon-exchange terms of the two-pion-exchange interaction. The results for V_j^{PS} and V_j^{PV} are the same as before, except that in this case the relevant variable is $(q')^2=(p_1-p_2')^2$ instead of $q^2=(p_1-p_1')^2$.

VI. SUMMARY AND DISCUSSION

Starting from an effective chiral Lagrangian describing the interaction of nucleons and pions, and determining the constants M and λ in Eq. (2.1) so that the known values of the nucleon mass and pion-nucleon coupling constant are reproduced, we have calculated the (uncorrelated) two-pion-exchange contribution to the nucleon-nucleon force. In carrying out this program, we

made a systematic expansion of the Lagrangian to the lowest orders in $1/f_\pi$, keeping all the relevant terms of order f_π^{-2} . We then isolated the various tensorial parts of the interaction in the isoscalar sector, and subtracted from that the contribution that arises from the iteration of the Born term of the single pion-exchange process in the Bethe-Salpeter equation. The resulting potentials describe the *irreducible* two-pion-exchange contribution to the NN isoscalar amplitude at one-loop order.

Our numerical results show that the content of the irreducible two-pion-exchange interaction, in the isoscalar sector, is mainly an attractive pseudoscalar potential that would tend to cancel out the repulsive potential due to the exchange of the physical η particle. There is also a small repulsive vector potential and in the case of the pseudovector coupling scheme, we found that about 25% of the empirical σ -meson scalar potential may originate from this process. We did not find any significant axial vector or tensor interactions in either coupling scheme.

As noted earlier in this work, we will have to provide a model for correlated two-pion-exchange process in order to extend the analysis given here. Correlated two-pion-exchange processes have been considered in studies based upon the use of dispersion relations [3,4]. In those studies the $\bar{N}N \rightarrow \pi\pi$ amplitude receives important contributions from π - π rescattering terms, which are expressed in terms of the on-shell $\pi\pi$ scattering amplitude. We hope to use the insight gained in the studies based upon the use of dispersion relations in further developments of our model.

Our analysis represents a first step in a program whose aim is to provide a relation between a chiral Lagrangian and the boson-exchange model of nuclear forces. We may use that relation to obtain a deeper understanding of the relativistic Brueckner–Hartree-Fock formalism [14], for example. Studies made using the Brueckner–Hartree-Fock theory may be understood as involving a two-step process: One starts with a Lagrangian that provides a nonlinear representation of chiral symmetry and then one replaces that Lagrangian with another effective Lagrangian that contains several auxiliary fields. The second of these Lagrangians, which we may identify with the Lagrangian of the OBEP model, may be studied in the “ladder approximation.” That is, one identifies irreducible one-boson-exchange interactions that may be iterated in a relativistic two-body equation [2]. As a next step, one constructs nuclear matter reaction matrices and proceeds to carry out a calculation of the properties of nuclear matter. As an alternate, we may also study the Nambu–Jona-Lasinio model and consider the coupling of the σ meson of that model and the two-pion continuum. Results of that program will be described in a future publication. The full implementation of these procedures may provide some understanding of the role of chiral symmetry when a field-theoretic formalism is used to study the nuclear many-body problem.

This work was supported in part by a grant from the National Science Foundation and by the PSC-CUNY Faculty Award Program.

-
- [1] R. Machleidt, K. Holinde, and Ch. Elster, *Phys. Rep.* **149**, 2 (1987). See Sec. V of this work for a discussion of two-pion-exchange contributions to the nucleon-nucleon force.
- [2] R. Machleidt, in *Advances in Nuclear Physics*, edited by J. W. Negele and E. Vogt (Plenum, New York, 1989), Vol. 19, p. 189.
- [3] J. W. Durso, A. D. Jackson, and B. J. Verwest, *Nucl. Phys.* **A345**, 471 (1980); J. W. Durso, M. Saavela, G. E. Brown, and A. D. Jackson, *ibid.* **A278**, 445 (1977).
- [4] W. Lin and B. D. Serot, *Nucl. Phys.* **A512**, 637 (1990).
- [5] V. Bernard, Ulf-G. Meissner, and I. Zahed, *Phys. Rev. Lett.* **59**, 966 (1987). See also *Phys. Rev. D* **36**, 819 (1987), for a discussion of the temperature and density dependence of the pion decay constant and the hadronic mass gap.
- [6] See, for example, B. D. Serot and J. D. Walecka, in *Advances in Nuclear Physics*, edited by J. Negele and E. Vogt (Plenum, New York, 1986), Vol. 16.
- [7] T. D. Cohen, R. J. Furnstahl, and D. K. Greigel, *Phys. Rev. C* **45**, 1881 (1992).
- [8] M. Lutz, S. Klimt, and W. Weise, *Nucl. Phys.* **A542**, 521 (1992).
- [9] L. S. Celenza, A. Pantziris, C. M. Shakin, and Wei-Dong Sun, *Phys. Rev. C* **45**, 2015 (1992).
- [10] L. S. Celenza, A. Pantziris, C. M. Shakin, and Wei-Dong Sun, *Phys. Rev. C* **46**, 571 (1992).
- [11] J. Gasser, H. Leutwyler, and M. E. Sainio, *Phys. Lett. B* **253**, 260 (1991).
- [12] B. D. Serot and J. D. Walecka, in *Advances in Nuclear Physics*, edited by J. W. Negele and E. Vogt (Plenum, New York, 1986), Vol. 16.
- [13] See, for example, S. J. Wallace, *Annu. Rev. Nucl. Part. Sci.* **37**, 267 (1987).
- [14] L. S. Celenza and C. M. Shakin, *Relativistic Nuclear Physics: Theories of Structure and Scattering* (World Scientific, Singapore, 1986).
- [15] V. Thorrsen and I. Zahed, *Phys. Rev. C* **45**, 965 (1992); M. Oka, *Phys. Rev. Lett.* **66**, 1019 (1991); H. Yamagishi and I. Zahed, *Phys. Rev. D* **43**, 891 (1991); T. S. Walhout and J. Wambach, *Phys. Rev. Lett.* **67**, 314 (1990).
- [16] K. Kang and A. Pantziris, *Phys. Rev. D* **43**, 241 (1991).
- [17] M. L. Goldberger, M. T. Grisaru, S. W. McDowell, and D. Y. Wong, *Phys. Rev.* **120**, 2250 (1960).
- [18] H. Georgi, *Weak Interactions and Modern Particle Theory* (Benjamin/Cummings, Menlo Park, 1984).
- [19] G. E. Brown and A. D. Jackson, *The Nucleon-Nucleon Interaction* (North-Holland, Amsterdam, 1976).
- [20] Further details concerning these calculations may be found in L. S. Celenza, A. Pantziris, and C. M. Shakin, Brooklyn College Report BCCNT 92/041/220R, 1992 (unpublished).